

HOSM Block Control of SPIM

Guillermo J. Rubio¹, Juan Diego Sánchez-Torres², José M. Cañedo³, and Alexander G. Loukianov⁴

¹⁻⁴ Department of Electrical Engineering, CINVESTAV Unidad Guadalajara, 45015 México
e-mail: [grubio¹, dsanchez², josec³, louk⁴]@gdl.cinvestav.mx

Abstract—In the continuation of authors' studies on control and estimation methods for Single-Phase Induction Motor (SPIM), a new observer-based controller using High Order Sliding Mode (HOSM) algorithms is proposed here. This observer-controller scheme only uses measurements of the rotor speed and stator currents. The complete scheme is robust to uncertainties in the rotor resistance, and a bounded time-varying load torque.

Keywords: Sliding Mode Control; Single-Phase Induction Motors (SPIM); Robust Control; Nonlinear Systems.

I. INTRODUCTION

The aim of this paper is to present an observer-based controller using second order Sliding Mode (SM) algorithms. The idea of use a second order SM controller for SPIM was introduced in [1]. Here, using measurements of currents and rotor speed, the controller induces a linear stable dynamics on the rotor flux and speed variables. In addition, the load torque is assumed as a slowly varying quantity which is estimated, jointly to the fluxes, using an state observer. No variation on the rotor resistance was considered in the mentioned approach.

In this article, a second-order SM observer is designed to estimate the fluxes. It uses the similarity between the natural form of the flux and the currents and the *Super-Twisting* algorithm structure [2]. Besides, a robust controller against, both *matched* and *unmatched*, perturbations is synthesized. The controller is calculated driving the system to the *Nonlinear Block Controllable Form* [3] and using quasi-continuous SM [4] surfaces as in [5].

The use of the proposed method allows to avoid the estimation of the load torque. In addition, its robustness permits to overcome the uncertainty due to the rotor resistance variations, improving the tracking accuracy.

In the following, Section II provides the considered model of the SPIM. Sections III and IV describe the proposed observer and controllers, including a detailed analysis of stability and robustness. The successful simulations are presented in section V. Finally, in Section VI the conclusions are given.

II. MATHEMATICAL MODEL FOR THE SPIM SYSTEM INCLUDING RESISTANCE VARIATIONS

A. Dynamic Equations

The dynamic model of the SPIM is the unsymmetrical 2-phase induction machine (a, b), in the variables of circuit elements with a transformation to a stationary of reference known as ($\alpha - \beta$) transformation, [6].

From this representation, the single phase induction motor scheme, in $\alpha\beta$ -axis, with the stator current and the rotor flux as the state variables, is presented in Fig. 1.

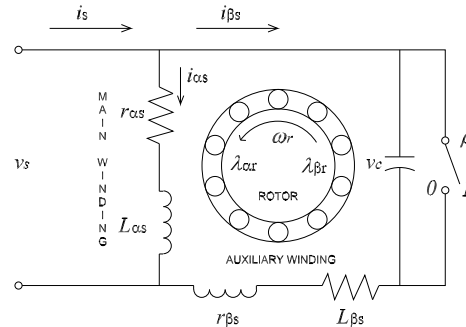


Fig. 1: Single phase induction motor

and its dynamic equations are given by

$$\begin{aligned}
 \frac{d\omega_r}{dt} &= d_1 d_2 (\lambda_{\beta r} i_{\alpha s} - \lambda_{\alpha r} i_{\beta s}) - d_2 T_L \\
 \frac{d\lambda_{\alpha r}}{dt} &= -a_3 \lambda_{\alpha r} + n_p \omega_r \lambda_{\beta r} + a_4 i_{\alpha s} \\
 \frac{d\lambda_{\beta r}}{dt} &= -n_p \omega_r \lambda_{\alpha r} - a_3 \lambda_{\beta r} + a_4 i_{\beta s} \\
 \frac{di_{\alpha s}}{dt} &= -c_1 a_1 i_{\alpha s} + c_1 c_4 \lambda_{\alpha r} - c_1 c_3 n_p \omega_r \lambda_{\beta r} + c_1 v_{\alpha s} \\
 \frac{di_{\beta s}}{dt} &= -c_2 a_2 i_{\beta s} + c_2 c_4 \lambda_{\beta r} + c_2 c_3 n_p \omega_r \lambda_{\alpha r} + c_2 v_{\beta s}
 \end{aligned} \tag{1}$$

where $\lambda_{\alpha r}$ and $\lambda_{\beta r}$ are the rotor magnetic-flux-linkage components, respectively, $i_{\alpha s}$ and $i_{\beta s}$ are the stator current components, respectively, $v_{\alpha s}$ and $v_{\beta s}$ are the voltage of the main and auxiliary stator windings, respectively, ω_r is the rotor speed, n_p is the number of pole pairs, T_L is the load torque, respectively. The model (1) constants a_i and c_i , ($i = 1, \dots, 4$) depend on the motor parameters and are given by $a_1 = R_{\alpha s} + \frac{R_r L_m^2}{L_s^2}$,

$a_2 = R_{\beta_s} + \frac{R_r L_m^2}{L_r^2}$, $a_3 = \frac{R_r}{L_r}$, $a_4 = \frac{R_r L_m}{L_r}$, $c_1 = \frac{L_r}{L_{\alpha_s} L_r - L_m^2}$, $c_2 = \frac{L_r}{L_{\beta_s} L_r - L_m^2}$, $c_3 = \frac{L_m}{L_r}$, $c_4 = \frac{r_r L_m}{L_r^2}$, $d_1 = n_p \frac{L_m}{L_r}$ and $d_2 = \frac{n_p}{J}$; where R_{α_s} and R_{β_s} are the stator resistances, L_{α_s} and L_{β_s} are the inductances of the stator, R_r and L_r are the rotor resistance and inductance, respectively, J is the rotor moment of inertia, and L_m is the mutual inductance between the main and auxiliary windings. The load torque T_L is assumed to be an unknown and bounded variable.

In addition, the dynamics of the capacitor are represented by

$$dv_c/dt = \omega X_c i_{\beta_s} \quad (2)$$

where X_c is the capacitor reactance and $\omega = 2\pi f$, with f being the fundamental frequency. Using the relation between the voltages v_{α_s} and v_{β_s} in (1) of the form,

$$\begin{aligned} v_{\alpha_s} &= v_s \\ v_{\beta_s} &= n^{-1}v_s - v_c\rho \end{aligned} \quad (3)$$

where the switching parameter ρ is defined by

$$\rho = \begin{cases} 1 \\ 0 \end{cases} \Rightarrow \begin{cases} v_{\beta_s} = n^{-1}v_s - v_c \\ v_{\beta_s} = n^{-1}v_s \end{cases},$$

being $n^{-1}v_s$ as a referred voltage of the main winding to the auxiliary winding with $n = N_A/N_B$, where N_A is the number turns of main winding and N_B is the number turns of an auxiliary winding.

B. Inclusion of Resistance Variations

One of the most important variations during motor operations is that of the rotor resistance (due to temperature changes), with respect to the nominal values R_{r0} . The real value is

$$R_r(t) = R_{r0} + \Delta R_r(t),$$

with $\Delta R_r(t)$ an unknown but bounded function of time.

Hence, $a_{10} = \left(R_{\alpha_s} + R_{r0} \frac{L_m^2}{L_r^2}\right)$, $a_{20} = \left(R_{\beta_s} + R_{r0} \frac{L_m^2}{L_r^2}\right)$, $a_{30} = \frac{R_{r0}}{L_r}$, $a_{40} = \frac{R_{r0}}{L_r} L_m$ and, $c_{40} = \frac{R_{r0}}{L_r^2} L$ are the nominal values of $a_1(t) = a_{10} + \Delta a_1(t)$, $a_2(t) = a_{20} + \Delta a_2(t)$, $a_3(t) = a_{30} + \Delta a_3(t)$, $a_4(t) = a_{40} + \Delta a_4(t)$, and $c_4(t) = c_{40} + \Delta c_4(t)$, respectively. Here, the uncertainties in the parameters are $\Delta a_1(t) = \Delta a_2(t) = \frac{L_m^2}{L_r^2} \Delta R_r(t)$, $\Delta a_3(t) = \frac{1}{L_r} \Delta R_r(t)$, $\Delta a_4(t) = \frac{L_m}{L_r} \Delta R_r(t)$, and $\Delta c_4(t) = \frac{L_m}{L_r^2} \Delta R_r(t)$.

Therefore, the flux and current dynamics of the SPIM

model can be reformulated as follows

$$\begin{aligned} \frac{d\lambda_{\alpha r}}{dt} &= -a_{30}\lambda_{\alpha r} + n_p\omega_r\lambda_{\beta r} + a_{40}i_{\alpha s} + \wp_1(t) \\ \frac{d\lambda_{\beta r}}{dt} &= -n_p\omega_r\lambda_{\alpha r} - a_{30}\lambda_{\beta r} + a_{40}i_{\beta s} + \wp_2(t) \\ \frac{di_{\alpha s}}{dt} &= -c_1a_{10}i_{\alpha s} + c_1c_{40}\lambda_{\alpha r} - c_1c_3n_p\omega_r\lambda_{\beta r} \\ &\quad + c_1v_{\alpha s} + \wp_3(t) \\ \frac{di_{\beta s}}{dt} &= -c_2a_{20}i_{\beta s} + c_2c_{40}\lambda_{\beta r} + c_2c_3n_p\omega_r\lambda_{\alpha r} \\ &\quad + c_2v_{\beta s} + \wp_4(t) \end{aligned} \quad (4)$$

with the unknown terms $\wp_1(t) = -\Delta a_3(t)\lambda_{\alpha r} + \Delta a_4(t)i_{\alpha s}$, $\wp_2(t) = -\Delta a_3(t)\lambda_{\beta r} + \Delta a_4(t)i_{\beta s}$, $\wp_3(t) = \Delta c_4(t)c_1\lambda_{\alpha r} - \Delta a_1(t)c_1i_{\alpha s}$, and $\wp_4(t) = \Delta c_4(t)c_2\lambda_{\beta r} - \Delta a_2(t)c_2i_{\beta s}$.

III. SECOND ORDER SLIDING MODE OBSERVER FOR ROTOR FLUXES

Having the rotor speed ω_r and stator current $i_{\alpha s}$ and $i_{\beta s}$ measurements only, in this section a sliding mode super-twisting observer is designed to estimate the rotor flux.

A. Observer Design

Consider the following transformation:

$$\begin{aligned} \lambda_{\alpha r}^* &= \lambda_{\alpha r} - l_1 i_{\alpha s} \\ \lambda_{\beta r}^* &= \lambda_{\beta r} - l_2 i_{\beta s} \end{aligned} \quad (5)$$

where l_1 and l_2 are the transformation gains to be chosen later. Using (5), the flux and current dynamics (4) are represented in new variables $\lambda_{\alpha r}^*$ and $\lambda_{\beta r}^*$ with the unknown terms of the form

$$\begin{aligned} \dot{\lambda}_{\alpha r}^* &= -l_{11}\lambda_{\alpha r}^* + l_{12}n_p\omega_r\lambda_{\beta r}^* + \varsigma_{11}n_p\omega_r i_{\beta s} + \varsigma_{12}i_{\alpha s} \\ &\quad - \varphi_1 v_{\alpha s} - l_1 \wp_3 + \wp_1 \\ \dot{\lambda}_{\beta r}^* &= -l_{21}\lambda_{\beta r}^* - l_{22}n_p\omega_r\lambda_{\alpha r}^* - \varsigma_{21}n_p\omega_r i_{\alpha s} + \varsigma_{22}i_{\beta s} \\ &\quad - \varphi_2 v_{\beta s} - l_2 \wp_4 + \wp_2 \\ \dot{i}_{\alpha s} &= -\vartheta_{11}i_{\alpha s} - \vartheta_{12}n_p\omega_r i_{\beta s} - \varphi_3 n_p\omega_r \lambda_{\beta r}^* + \varphi_4 \lambda_{\alpha r}^* \\ &\quad + c_1 v_{\alpha s} + \wp_3 \\ \dot{i}_{\beta s} &= -\vartheta_{21}i_{\beta s} + \vartheta_{22}n_p\omega_r i_{\alpha s} + \varphi_5 n_p\omega_r \lambda_{\alpha r}^* + \varphi_6 \lambda_{\beta r}^* \\ &\quad + c_2 v_{\beta s} + \wp_4 \end{aligned} \quad (6)$$

where $l_{11} = a_{30} + l_1 c_1 c_{40}$, $l_{12} = 1 + l_1 c_1 c_3$, $l_{21} = a_{30} + l_2 c_2 c_{40}$, $l_{22} = 1 + l_2 c_2 c_3$, $\varsigma_{11} = l_{12} l_2$, $\varsigma_{12} = a_{40} - l_{11} l_1 + l_1 c_1 a_{10}$, $\varsigma_{21} = l_{22} l_1$, $\varsigma_{22} = a_{40} - l_{21} l_2 + l_2 c_2 a_{20}$, $\vartheta_{11} = c_1 a_{10} - l_1 c_1 c_{40}$, $\vartheta_{12} = l_2 c_1 c_3$, $\vartheta_{21} = c_2 a_{20} - l_2 c_2 c_{40}$, $\vartheta_{22} = l_1 c_2 c_3$, $\varphi_1 = l_1 c_1$, $\varphi_2 = l_2 c_2$, $\varphi_3 = c_1 c_3$, $\varphi_4 = c_1 c_{40}$, $\varphi_5 = c_2 c_3$, and $\varphi_6 = c_2 c_{40}$.

Based on (6), and defining $\hat{\lambda}_{\alpha r}^*$, $\hat{\lambda}_{\beta r}^*$, $\hat{i}_{\alpha s}$, and $\hat{i}_{\beta s}$ as the estimates of $\lambda_{\alpha r}^*$, $\lambda_{\beta r}^*$, $i_{\alpha s}$, and $i_{\beta s}$, respectively, a

nonlinear observer is designed as follows:

$$\begin{aligned}
\dot{\hat{\lambda}}_{\alpha r}^* &= -l_{11}\hat{\lambda}_{\alpha r}^* + l_{12}n_p\omega_r\hat{\lambda}_{\beta r}^* + \varsigma_{11}n_p\omega_r\hat{i}_{\beta s} + \varsigma_{12}\hat{i}_{\alpha s} \\
&\quad - \varphi_1 v_{\alpha s} + \frac{k_{2\alpha}}{\varphi_4} \text{sign}(\tilde{i}_{\alpha s}) \\
\dot{\hat{\lambda}}_{\beta r}^* &= -l_{21}\hat{\lambda}_{\beta r}^* - l_{22}n_p\omega_r\hat{\lambda}_{\alpha r}^* - \varsigma_{21}n_p\omega_r\hat{i}_{\alpha s} + \varsigma_{22}\hat{i}_{\beta s} \\
&\quad - \varphi_2 v_{\beta s} + \frac{k_{2\beta}}{\varphi_6} \text{sign}(\tilde{i}_{\beta s}) \\
\dot{\hat{i}}_{\alpha s} &= -\vartheta_{11}\hat{i}_{\alpha s} - \vartheta_{12}n_p\omega_r\hat{i}_{\beta s} - \varphi_3 n_p\omega_r\hat{\lambda}_{\beta r}^* + \varphi_4 \hat{\lambda}_{\alpha r}^* \\
&\quad + c_1 v_{\alpha s} + k_{1\alpha} |\tilde{i}_{\alpha s}|^{\frac{1}{2}} \text{sign}(\tilde{i}_{\alpha s}) + k_{3\alpha} \tilde{i}_{\alpha s} \\
\dot{\hat{i}}_{\beta s} &= -\vartheta_{21}\hat{i}_{\beta s} + \vartheta_{22}n_p\omega_r\hat{i}_{\alpha s} + \varphi_5 n_p\omega_r\hat{\lambda}_{\alpha r}^* + \varphi_6 \hat{\lambda}_{\beta r}^* \\
&\quad + c_2 v_{\beta s} + k_{1\beta} |\tilde{i}_{\beta s}|^{\frac{1}{2}} \text{sign}(\tilde{i}_{\beta s}) + k_{3\beta} \tilde{i}_{\beta s}
\end{aligned} \tag{7}$$

where $\tilde{i}_{\alpha s} = i_{\alpha s} - \hat{i}_{\alpha s}$, and $\tilde{i}_{\beta s} = i_{\beta s} - \hat{i}_{\beta s}$ are the estimation errors of $i_{\alpha s}$, and $i_{\beta s}$, respectively. With $k_{i\alpha}, k_{i\beta} > 0$ for $i = 1, 2, 3$.

As a result, the rotor flux estimates $\hat{\lambda}_{\alpha r}$ and $\hat{\lambda}_{\beta r}$ are obtained as $\hat{\lambda}_{\alpha r} = \hat{\lambda}_{\alpha r}^* + l_1 i_{\alpha s}$ and $\hat{\lambda}_{\beta r} = \hat{\lambda}_{\beta r}^* + l_2 i_{\beta s}$.

B. Convergence Analysis

Defining the additional the estimation errors $\tilde{\lambda}_{\alpha r}^* = \lambda_{\alpha r}^* - \hat{\lambda}_{\alpha r}^*$, and $\tilde{\lambda}_{\beta r}^* = \lambda_{\beta r}^* - \hat{\lambda}_{\beta r}^*$. Then, from (7), the observer error dynamics are obtained on the form

$$\begin{aligned}
\dot{\tilde{i}}_{\alpha s} &= -k_{1\alpha} |\tilde{i}_{\alpha s}|^{\frac{1}{2}} \text{sign}(\tilde{i}_{\alpha s}) - (k_{3\alpha} + \vartheta_{11}) \tilde{i}_{\alpha s} \\
&\quad + \varphi_4 \tilde{\lambda}_{\alpha r}^* + \Delta_{1\alpha} \\
\dot{\tilde{\lambda}}_{\alpha r}^* &= -\frac{k_{2\alpha}}{\varphi_4} \text{sign}(\tilde{i}_{\alpha s}) + \Delta_{2\alpha} \\
\dot{\tilde{i}}_{\beta s} &= -k_{1\beta} |\tilde{i}_{\beta s}|^{\frac{1}{2}} \text{sign}(\tilde{i}_{\beta s}) - (k_{3\beta} + \vartheta_{21}) \tilde{i}_{\beta s} \\
&\quad + \varphi_6 \tilde{\lambda}_{\beta r}^* + \Delta_{1\beta} \\
\dot{\tilde{\lambda}}_{\beta r}^* &= -\frac{k_{2\beta}}{\varphi_6} \text{sign}(\tilde{i}_{\beta s}) + \Delta_{2\beta}
\end{aligned} \tag{8}$$

where $\Delta_{1\alpha} = -\vartheta_{12}n_p\omega_r\tilde{i}_{\beta s} - \varphi_3 n_p\omega_r\tilde{\lambda}_{\beta r}^* + \wp_3$, $\Delta_{2\alpha} = -l_{11}\tilde{\lambda}_{\alpha r}^* + l_{12}n_p\omega_r\tilde{\lambda}_{\beta r}^* - l_1\wp_3 + \wp_1$, $\Delta_{1\beta} = \vartheta_{22}n_p\omega_r\tilde{i}_{\alpha s} + \varphi_5 n_p\omega_r\tilde{\lambda}_{\alpha r}^* + \wp_4$, and $\Delta_{2\beta} = -l_{21}\tilde{\lambda}_{\beta r}^* - l_{22}n_p\omega_r\tilde{\lambda}_{\alpha r}^* + l_2\wp_4 + \wp_2$.

Following the Lyapunov approach proposed in [7], lets assume that $|\Delta_{1\alpha}|, |\dot{\Delta}_{1\alpha}| < \delta_{1\alpha}$; $|\Delta_{2\alpha}| < \delta_{2\alpha}$ and $|\Delta_{1\beta}|, |\dot{\Delta}_{1\beta}| < \delta_{1\beta}$; $|\Delta_{2\beta}| < \delta_{2\beta}$. Then, choosing $k_{1\alpha} > 0$, $k_{1\beta} > 0$, $k_{2\alpha} > \frac{k_{1\alpha}\delta_{2\alpha} + \frac{1}{8}\delta_{2\alpha}^2}{2(\frac{1}{8}k_{1\alpha} - \delta_{2\alpha})} k_{1\alpha}$, $k_{2\beta} > \frac{k_{1\beta}\delta_{2\beta} + \frac{1}{8}\delta_{2\beta}^2}{2(\frac{1}{8}k_{1\beta} - \delta_{2\beta})} k_{1\beta}$, $k_{3\alpha} > \frac{17}{8}\delta_{1\alpha} - \vartheta_{11}$, and $k_{3\beta} > \frac{17}{8}\delta_{1\beta} - \vartheta_{21}$; the estimation error converges to zero in finite time.

IV. SLIDING MODE CONTROLLER DESIGN

Provided that the currents and speed vector are measured and the rotor flux estimated, the objective here is to design a SM controller which can effectively track the desired speed ω_{ref} and the module to the square of the rotor flux ϕ_{ref} reference signals by means of the

continuous basic control v_s and auxiliary control ρ as a discontinuous function.

A. Sliding Manifold Design

As first step, the model (α, β) of the SPIM (1) is transformed, here $\phi = |\psi|^2 = \hat{\lambda}_{\alpha r}^2 + \hat{\lambda}_{\beta r}^2$ is the module to the square of rotor flux. After that, it is defined the state variables as

$$x_1 = \begin{bmatrix} \omega_r \\ \phi \end{bmatrix} \quad \text{and} \quad x_2 = \begin{bmatrix} i_{\alpha s} \\ i_{\beta s} \end{bmatrix}.$$

Then, the system (1) can be represented in the so-called Nonlinear Block Control form with perturbation, [3], which consists of two blocks:

$$\dot{x}_1 = f_1(\phi) + B_1(\hat{\lambda}_r) x_2 + D_1 T_L + \wp_a(t) \tag{9}$$

$$\dot{x}_2 = f_2(\omega_r, \hat{\lambda}_r, i_s) + B_2 u + \wp_b(t) \tag{10}$$

$$\begin{aligned}
\text{where } f_1(\phi) &= \begin{bmatrix} f_{11} \\ f_{12} \end{bmatrix} = \begin{bmatrix} 0 \\ -2a_{30}\phi \end{bmatrix}, \\
B_1(\hat{\lambda}_r) &= \begin{bmatrix} d_1 d_2 \hat{\lambda}_{\beta r} & -d_1 d_2 \hat{\lambda}_{\alpha r} \\ 2a_{40} \hat{\lambda}_{\alpha r} & 2a_{40} \hat{\lambda}_{\beta r} \end{bmatrix}, \quad \hat{\lambda}_r = (\hat{\lambda}_{\alpha r}, \hat{\lambda}_{\beta r}), \\
D_1 &= \begin{bmatrix} -d_2 \\ 0 \end{bmatrix}, \quad \wp_a(t) = \begin{bmatrix} 0 \\ 2\wp_1(t) \hat{\lambda}_{\alpha r} + 2\wp_2(t) \hat{\lambda}_{\beta r} \end{bmatrix}, \\
\wp_b(t) &= \begin{bmatrix} \wp_3(t) \\ \wp_4(t) \end{bmatrix}, \quad f_2 = \begin{bmatrix} f_{21} - a_{10} c_1 i_{\alpha s} \\ f_{22} - a_{20} c_2 i_{\beta s} \end{bmatrix}, \\
f_{21} &= c_1 c_{40} \hat{\lambda}_{\alpha r} - c_1 c_3 \omega_r \hat{\lambda}_{\beta r}, \quad B_2 = \begin{bmatrix} c_1 & 0 \\ 0 & c_2 \end{bmatrix}, \\
f_{22} &= c_2 c_3 \omega_r \hat{\lambda}_{\alpha r} + c_2 c_{40} \hat{\lambda}_{\beta r}, \\
\text{and } u &= \begin{bmatrix} v_{\alpha s} \\ v_{\beta s} \end{bmatrix} = \begin{bmatrix} v_s \\ n^{-1} v_s - v_{c\rho} \end{bmatrix}.
\end{aligned}$$

Setting the tracking error as $z_1 = [z_{11}, z_{12}]^T = [\omega_r - \omega_{ref}(t), \phi - \phi_{ref}(t)]^T$, and using the block control technique, [3], the desired value x_{2des} for the virtual control x_2 in the first block (9) is proposed of the form

$$x_{2des} = B_1^{-1}(\hat{\lambda}_r) (-f_1(\phi) - K_0 z_0 - K_1 z_1 + \nu) \tag{11}$$

$$\begin{aligned}
\text{where } K_0 &= \begin{bmatrix} k_{01} & 0 \\ 0 & k_{02} \end{bmatrix}, \quad K_1 = \begin{bmatrix} k_1 & 0 \\ 0 & k_2 \end{bmatrix}, \\
\nu &= [\nu_1, \nu_2]^T, \quad \dot{\nu} = \begin{bmatrix} -k_{a1} \frac{\dot{z}_{11} + |z_{11}|^{\frac{1}{2}} \text{sign}(z_{11})}{|z_{11}| + |z_{11}|^{\frac{1}{2}}} \\ -k_{a2} \frac{\dot{z}_{12} + |z_{12}|^{\frac{1}{2}} \text{sign}(z_{12})}{|z_{12}| + |z_{12}|^{\frac{1}{2}}} \end{bmatrix}, \quad z_0 = \\
& [z_{01}, z_{02}]^T, \quad \dot{z}_0 = z_1, \quad \text{and } k_{a1}, k_{a2}, k_{01}, k_{02}, k_1, k_2 > 0.
\end{aligned}$$

B. Inducing Sliding Modes

Let the sliding variable z_2 defined now as follows

$$z_2 = x_2 - x_{2des} \tag{12}$$

where $z_2 = [z_{21}, z_{22}]^T$, $z_{21} = i_{\alpha s} - i_{\alpha s}^{des}$, $z_{22} = i_{\beta s} - i_{\beta s}^{des}$; with

$$\begin{aligned} i_{\alpha s}^{des} &= \frac{1}{\phi} \left[\frac{\hat{\lambda}_{\beta r}}{d_1 d_2} (-k_1 z_{11} - k_{01} z_{01} + \nu_1) \right. \\ &\quad \left. + \frac{\hat{\lambda}_{\alpha r}}{2a_{40}} (2a_{30}\phi - k_2 z_{12} - k_{02} z_{02} + \nu_2) \right] \\ i_{\beta s}^{des} &= \frac{1}{\phi} \left[-\frac{\hat{\lambda}_{\alpha r}}{d_1 d_2} (-k_1 z_{11} - k_{01} z_{01} + \nu_1) \right. \\ &\quad \left. + \frac{\hat{\lambda}_{\beta r}}{2a_{40}} (2a_{30}\phi - k_2 z_{12} - k_{02} z_{02} + \nu_2) \right] \end{aligned}$$

In the slave loop ($i_{\alpha s}, i_{\beta s}$), first, the basic control v_s will be formulated. To induce a sliding mode motion on the manifold $z_{21} = 0$ or $i_{\alpha s} = i_{\alpha s}^{des}$, the super-twisting SM control algorithm [2], is applied:

$$v_s = -\alpha_1 |z_{21}|^{1/2} \text{sign}(z_{21}) - \alpha_3 z_{21} + u_1 \quad (13)$$

with $\dot{u}_1 = -\alpha_2 \text{sign}(z_{21})$.

And to induce a quasi-sliding mode motion on the manifold $z_{22} = 0$ or $i_{\beta s} = i_{\beta s}^{des}$, the auxiliary control ρ is designed by means of the switching logic for the capacitor, chosen as follows

$$\rho = \begin{cases} 1 & \text{if } z_{22} > 0 \text{ and } v_c > 0 \\ 0 & \text{if } z_{22} > 0 \text{ and } v_c < 0 \\ 0 & \text{if } z_{22} < 0 \text{ and } v_c > 0 \\ 1 & \text{if } z_{22} < 0 \text{ and } v_c < 0 \end{cases}$$

that results in

$$\rho = 0.5 \text{sign}(z_{22} v_c) + 0.5. \quad (14)$$

In order to analyze the stability of the reaching phase stage, lets substitute the control law (13) in (10). Hence, the closed-loop system becomes

$$\begin{aligned} \dot{z}_{21} &= f_s - c_1 \alpha_1 |z_{21}|^{1/2} \text{sign}(z_{21}) - c_1 \alpha_3 z_{21} + c_1 u_1 \\ \dot{u}_1 &= -\alpha_2 \text{sign}(z_{21}) \end{aligned} \quad (15)$$

with $f_s = f_{21} - a_{10} c_1 i_{\alpha s}^{des} - \frac{d i_{\alpha s}^{des}}{dt} + \wp_3(t)$, $\alpha_1 > 0$, $\alpha_2 > 0$, and $\alpha_3 > 0$ where the term f_s , considered as a perturbation in (15), is bounded by

$$|f_s| \leq \delta_1 |z_{21}| + \delta_2 \quad (16)$$

for constants $\delta_1 > 0$ and $\delta_2 > 0$. Choose the control gains α_1 , α_2 , and α_3 in (13) such that $\alpha_1 > 0$, $\alpha_2 > c_1 \alpha_1 \frac{(\delta_2 c_1 \alpha_1 + \frac{1}{2} \delta_2^2)}{2(\frac{1}{8} c_1 \alpha_1 - \delta_2)}$, and $\alpha_3 > \frac{17}{8} \delta_1$. Then, the state vector of the closed-loop system (15) reaches the manifold $z_{21} = 0$ in finite time [7].

In SM motion on the manifold $z_{21} = 0$, the equivalent value $v_{s,eq}$ [8], of the control v_s is calculated as a solution to $\dot{z}_{21} = 0$, (15) of the form

$$v_{s,eq} = c_1^{-1} f_s. \quad (17)$$

Substituting (17) in the equation (10) yields

$$\dot{z}_{22} = -a_{22} z_{22} + \bar{f}_{22}(\bar{z}) - c_2 v_c \rho \quad (18)$$

where $\bar{z} = [z_{11}, z_{12}, z_{22}]^T$, $a_{22} = a_2 c_2$ and $\bar{f}_{22}(\bar{z}) = f_{22} + c_2 (n c_1)^{-1} f_s - a_{22} i_{\beta s}^{des} - d i_{\beta s}^{des} / dt + \wp_4(t)$

Thus, to analyze the stability of (18) closed-loop by (14) the following quadratic Lyapunov function candidate is proposed:

$$V = \frac{1}{2} z_{22}^2. \quad (19)$$

In addition, the perturbation $g(\bar{z})$ is considered bounded by

$$\|\bar{f}_{22}(\bar{z})\| \leq \gamma_1 \|\bar{z}\| + \gamma_2, \quad \gamma_1 > 0, \gamma_2 > 0. \quad (20)$$

Then, the time derivative of (19) along the trajectories of (18) is calculated as

$$\dot{V} = -a_{22} z_{22}^2 + \bar{f}_{22}(\bar{z}) z_{22} - c_2 z_{22} v_c \rho. \quad (21)$$

Substituting (14) in (21) and using $z_{22} v_c \text{sign}(z_{22} v_c) = |z_{22} v_c|$, the derivative (21) becomes

$$\begin{aligned} \dot{V} &= -a_{22} z_{22}^2 + \bar{f}_{22}(\bar{z}) z_{22} - 0.5 c_2 (|z_{22} v_c| - z_{22} v_c) \\ &< -a_{22} |z_{22}|^2 + |\bar{f}_{22}(\bar{z})| |z_{22}| \end{aligned} \quad (22)$$

Using now (20) in (22) and adding and subtracting $(\alpha - \gamma_1) \beta |z_{22}|^2$, yields

$$\dot{V} \leq -(a_{22} - \gamma_1) (1 - \beta) |z_{22}|^2 \quad (23)$$

where $0 < \beta < 1$, $\forall |z_{22}| > \frac{\gamma_2}{(a_{22} - \gamma_1) \beta}$

Therefore, assuming that $a_{22} > \gamma_1$, a quasi-sliding motion is induced in the vicinity defined by $|z_{22}| \leq \delta_0$, $\delta_0 = \frac{\gamma_2}{(a_{22} - \gamma_1) \beta}$.

Finally, to limit the stator currents we propose the following logic for the sliding variables z_{21} and z_{22} :

$$\begin{aligned} z_{21} &= \begin{cases} i_{\alpha s} - i_{\alpha s}^{des} & \text{for } |i_{\alpha s}| \leq I_{\max} \\ i_{\alpha s} & \text{for } |i_{\alpha s}| > I_{\max} \end{cases} \\ z_{22} &= \begin{cases} i_{\beta s} - i_{\beta s}^{des} & \text{for } |i_{\beta s}| \leq I_{\max} \\ i_{\beta s} & \text{for } |i_{\beta s}| > I_{\max} \end{cases} \end{aligned}$$

where I_{\max} is a maximum admissible current value, $I_{\max} \approx 3 I_{\text{nom}}$, and I_{nom} is the nominal value of the current module.

This current limit provides maximum electrical torque produced by motor during the closed-loop transient process.

C. Sliding Mode Stability

The dynamics on the set $z_{21} = 0, |z_{22}| \leq \delta_0$ is given by

$$\dot{z}_{11} = -k_1 z_{11} - k_{11} z_{01} + \nu_1 + \Delta_1 \quad (24)$$

$$\dot{z}_{12} = -k_2 z_{12} - k_{12} z_{02} + \nu_2 + \Delta_2 \quad (25)$$

where $\Delta_1 = -d_2 T_L - \dot{\omega}_{ref}(t)$ and $\Delta_2 = 2\wp_1(t) \hat{\lambda}_{\alpha r} + 2\wp_2(t) \hat{\lambda}_{\beta r} - \dot{\phi}_{ref}(t)$.

Lets assume that $|\Delta_1|, |\dot{\Delta}_1| < \Delta_1^+$ and $|\Delta_2|, |\dot{\Delta}_2| < \Delta_2^+$, with $\Delta_1^+, \Delta_2^+ > 0$. Then, regarding Eq. (24), define $\xi_{11} = z_{11}$ and $\xi_{12} = \dot{z}_{11}$, with dynamics

$$\dot{\xi}_{11} = \xi_{12}$$

$$\dot{\xi}_{12} = -k_1 \xi_{12} - k_{11} \xi_{11} - k_{a1} \frac{\xi_{12} + |\xi_{11}|^{\frac{1}{2}} \text{sign}(\xi_{11})}{|\xi_{12}| + |\xi_{11}|^{\frac{1}{2}}} + \dot{\Delta}_1$$

therefore, if $k_{a1} > \Delta_1^+$, $(\xi_{11}, \xi_{12}) = (0, 0)$ in finite time [4]. Establishing a finite time sliding mode for the constraint $z_{11} = 0$ despite of the perturbation Δ_1 .

With the same analysis for the Eq. (25), the existence of a finite time sliding mode for the constraint $z_{12} = 0$ despite of the perturbation Δ_2 is demonstrated.

V. NUMERICAL SIMULATION RESULTS

In order to verify the effectiveness and efficiency of the proposed observer-based controller, numerical simulations are conducted using the Euler integration method with a time step $t_s = 1 \times 10^{-3}$.

Parameters and data of the SPIM are as follows, [6]: $H.P. = 0.25$, $V_s = 110$ V, $f = 60$ Hz, $n_p = 2$, $n = N_A/N_B = 1.18$, $r_{\alpha s} = 2.02$ Ω , $r_{\beta s} = 5.13$ Ω , $r_r = 4.12$ Ω , $L_m = 0.1772$ H, $L_{\alpha s} = 0.1846$ H, $L'_{\beta s} = 0.1833$ H, $L_r = 0.1828$ H, $J = 0.0146$ Kg-m², $I_{\max} = 15$ A, $C_{run} = 35$ μ F.

The controller gains are adjusted as $k_1 = k_2 = 500$, $k_{01} = k_{02} = 30$, $k_{a1} = k_{a2} = 5$, $\alpha_1 = 36$, and $\alpha_3 = 1$ the gains for the transformation are $l_1 = l_2 = 0.01$, finally the gains for the super-twisting observer are $k_{1\alpha} = 195$, $k_{1\beta} = 140$, $k_{3\alpha} = k_{3\beta} = 7000$, $k_{2\alpha} = k_{2\beta} = 0.02$, respectively.

For the simulation purposes, the initial conditions of the state variables are selected to zero. Tracking performance is verified for the two plant outputs: driving the square of rotor flux ϕ to a constant reference $\phi_{ref} = 0.15$, and for ω_r a speed profile, ω_{ref} , is proposed as follows:

- 1) The SPIM starts on repose with the reference speed on 100 rad/sec.
- 2) At the first second, a change of the speed reference – in ramp form – from 100 rad/sec to 120 rad/sec, is presented.
- 3) Finally, at 4 seconds, a change of the speed reference – in negative ramp form – from 120 rad/sec to 100 rad/sec, is presented.

In addition, the system is subject to disturbances. These disturbances are introduced as follows:

- 1) The SPIM starts on repose with a load torque of $0.5 + 0.1 \sin(2.5t)$ N-m.
- 2) At 2 seconds, a 30% increase in the value of the rotor resistance is presented.

The rotor speed tracking response is depicted in Fig. 2 which shows a good performance under the change of

the speed reference at $t = 1, 4$ sec., i.e. the speed tracking effect is achieved almost totally after 0.087 sec.

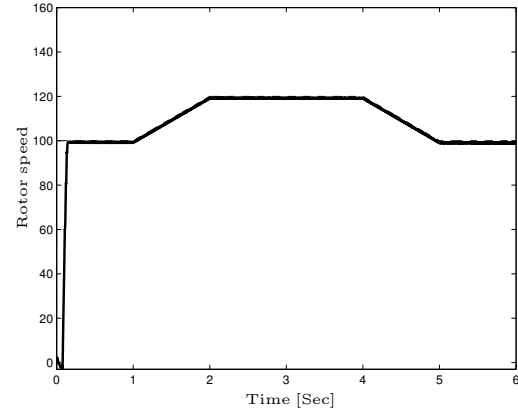


Fig. 2: Rotor speed ω_r and reference ω_{ref} .

The Figure 3 presents the module to the square of the rotor flux ϕ response; the module is maintained over the given reference.

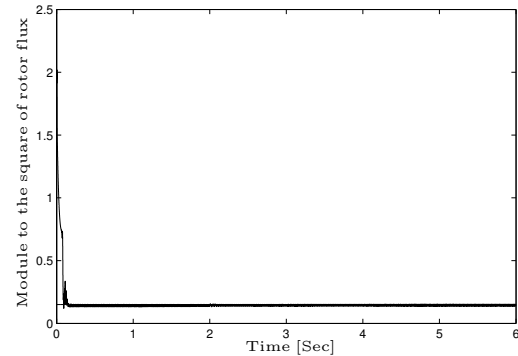


Fig. 3: Module to the square of rotor flux ϕ .

Errors of rotor flux are shown in Fig. 4, and they are zero.

The electromagnetic torque response is depicted in Fig. 5, showing that the torque has a high value 20 N-m during the interval $[0, 0.088]$ sec. This high value ensures a fast response of the speed (see Fig.2).

The result of the change in the value of the rotor resistance is shown as well, the typical oscillatory components of the second harmonic appear in the steady state due to the asymmetry of the auxiliary winding and main winding, see Figures 2, 3, and 5. However, the amplitude of these components has small values.

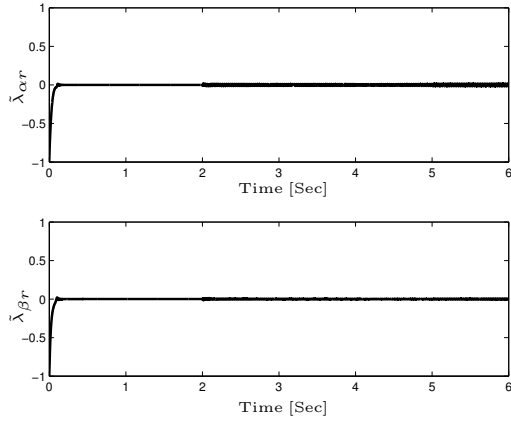


Fig. 4: Error of rotor flux in axis frame $\alpha \beta$.

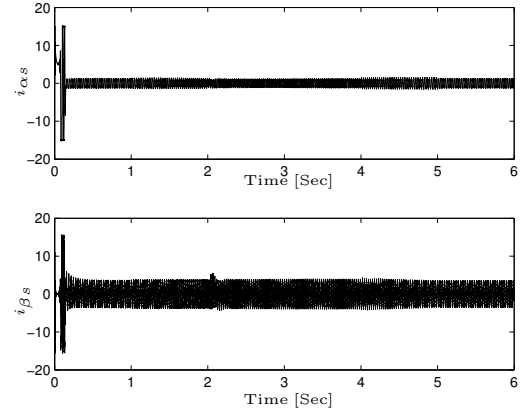


Fig. 6: Stator currents in axis frame $\alpha \beta$.

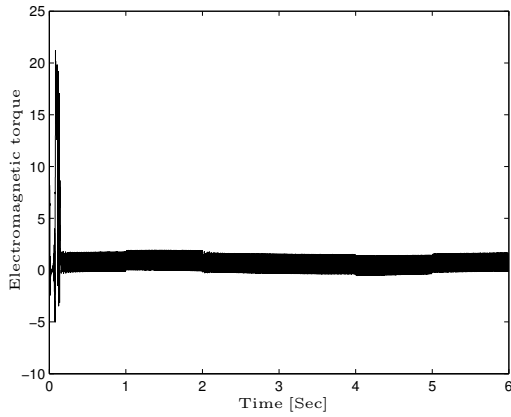


Fig. 5: Electromagnetic torque T_e .

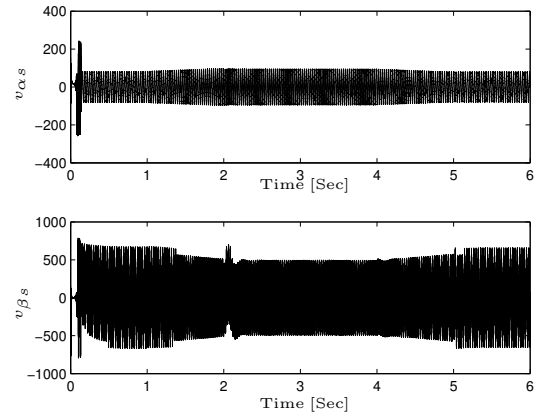


Fig. 7: Stator control voltages of axis $\alpha \beta$.

On the other hand, the stator currents (see Fig. 6) are in the appropriate range during the start ($0 < t < 0.2$) that corresponds to a desired control algorithm.

Finally, in Fig. 7, the responses of the voltages are presented, where $v_{\alpha s}$ as the super-twisting SM control and $v_{\beta s}$ as the discontinuous SM control.

VI. CONCLUSIONS

A control scheme based on the block control technique, quasi-continuous SM surfaces and second order SM super-twisting algorithm, was proposed to track the rotor angular speed ω_r and module to the square of rotor flux ϕ . In addition, a nonlinear second order SM observer was designed to estimate the rotor flux. Besides, the stability conditions of the closed-loop system with the proposed observer-based control was derived.

The simulation results have shown a robust performance of the designed controller with respect to the perturbations caused by the load torque. Moreover, the proposed controller ensures the constraints on the stator current.

REFERENCES

- [1] G. J. Rubio, J. M. Cañedo, A. G. Loukianov, and J. M. Reyes, "Second order sliding mode block control of single-phase induction motors," in *Proceedings of the 18th IFAC World Congress, Milan, Italy*, 2011.
- [2] A. Levant, "Sliding order and sliding accuracy in sliding mode control," *International Journal of Control*, vol. 58, no. 6, pp. 1247–1263, 1993.
- [3] A. Loukianov, "Robust block decomposition sliding mode control design," *Mathematical Problems in Engineering*, vol. 8, no. 4-5, pp. 349–365, 2002.
- [4] A. Levant, "Quasi-continuous high-order sliding-mode controllers," *IEEE Transactions on Automatic Control*, vol. 50, no. 11, pp. 1812–1816, 2005.
- [5] A. Estrada and L. Fridman, "Quasi-continuous HOSM control for systems with unmatched perturbations," *Automatica*, vol. 46, no. 11, pp. 1916 – 1919, 2010.
- [6] P. Krause, O. Wasynczuk, and S. Sudhoff, *Analysis of electric machinery and drive systems*, ser. IEEE Press series on power engineering, I. Press, Ed. IEEE Press, 2002.
- [7] J. A. Moreno and M. Osorio, "A Lyapunov approach to second-order sliding mode controllers and observers," in *Proc. 47th IEEE Conf. Decision and Control CDC 2008*, 2008, pp. 2856–2861.
- [8] V. Utkin, *Sliding modes in control and optimization*, ser. Communications and control engineering series. Springer-Verlag, 1992.